

Parametric scattering at the interface between two media

S. N. Kosolobov

Institute of Semiconductor Physics, Siberian Section, Academy of Sciences of the USSR

R. I. Sokolovskii

Moscow Institute of Steel and Alloys

(Submitted 22 May 1979)

Zh. Eksp. Teor. Fiz. 76, 816-823 (March 1979)

Emission of light induced by irradiation with an intense light beam (pumping) has been observed in lithium iodate crystals. The emitted light has a continuous spectrum lying in the Stokes region relative to the pumping frequency. The intensity of the radiation increases with increasing concentration of defects $\sim 10 \mu\text{m}$ in size and larger. In the absence of absorption, the spectral distribution of the radiation is the same as for parametric luminescence. In the presence of absorption at the ballast frequency, the spectrum of the radiation is determined by the frequency dependence of the absorption coefficient. The radiation is unpolarized and has no pronounced space-frequency characteristics. It is concluded that the investigated emission is due to parametric scattering of light at the interface between two media. A formula is derived for the spectral and angular dependence of the scattered light. Scattering indicatrices were measured at scattered-light wavelengths of 0.6 and 0.65 μm for thin plates pumped at a wavelength of 0.53 μm , and the results are presented. The indicatrices have two peaks, the positions of which are determined by the geometry of the interacting waves (the pumping wave and the field of the zero-point oscillations). The experimental results are in good agreement with the theory.

PACS numbers: 78.40.Ha

INTRODUCTION

Parametric luminescence (PL) was observed experimentally in 1967.^{1,2} This phenomenon consists of the decay, within the body of a crystal exhibiting quadratic nonlinearity, of a quantum of incident (pumping) light into two quanta of lower frequency ($\hbar\omega_p = \hbar\omega_s + \hbar\omega_i$) that satisfy the condition $\mathbf{k}_p = \mathbf{k}_s + \mathbf{k}_i$ of spatial synchronism. PL contains a broad spectrum of frequencies lying below the pumping frequency. The frequency of the scattered light is strictly connected to the direction of observation, and its spectral intensity in the region in which the crystal is transparent to the wavelengths of the interacting fields is proportional to the volume of the crystal occupied by the pumping field.^{3,4} In PL the scattered radiation is the result of interference enhancement of secondary waves emitted by elementary dipoles. Disturbing the synchronism condition, e.g., by altering the orientation of the crystal, is equivalent to disturbing the phase matching of the secondary waves and leads to interference quenching of the scattered light for the same physical reason as in the case of Rayleigh scattering.⁵

In an inhomogeneous medium, complete interference quenching does not take place⁵; the decay process is observed again,⁶ but it no longer has any fixed space-frequency characteristic.⁶ Experimental studies⁶ have shown that parametric decay of photons with violation of the synchronism condition takes place in crystals having a high density of inclusions with sizes of the order of 10 μm . From this one can conclude that the scattered radiation is actually formed at the inclusion boundaries. This raised the question of investigating the parametric scattering of light at the plane interface between two media, and in particular, at the interface between the vacuum and a crystal exhibiting quadratic

nonlinearity.

The radiation from a layer of elementary emitters of the order of a wavelength thick next to the interface between the media is not quenched by neighboring layers⁷ and contributes to the scattered radiation arising from the parametric decay of the pumping light. Because the intensity of the PL is proportional to the volume of the crystal, the spectral intensity of the scattering at the interface between the media should be smaller than the PL by a factor of about a/λ , where λ is the wavelength and a is the thickness of the crystal. In this case the conversion factor per unit solid angle and for a unit spectral interval can be estimated on the basis of experimental data;² it turns out to be of the order of 10^{-15} cm/sr. Despite the smallness of the conversion factor, the effect can be observed by using photon counters.

The present work is devoted to a theoretical and experimental study of this phenomenon.

THEORETICAL PART

The mixing^{8,9} of the pumping wave with the fluctuation field¹⁰ in a crystal having quadratic nonlinearity results in waves of nonlinear polarization

$$\mathbf{P} = \mathbf{P}_0 e^{i(\omega t - \mathbf{k}r)}, \quad \mathbf{P}_0 = \hat{\chi}(\omega = \omega_p - \omega_i) \mathbf{E}_0 \mathbf{E}_i, \quad (1)$$

whose radiation gives rise to the scattered light. Here $\hat{\chi}$ is the nonlinear-susceptibility tensor of the crystal; \mathbf{E}_0 and \mathbf{E}_i are the amplitudes of the electric fields of the pumping wave and the fluctuation field; and $\omega = \omega_p - \omega_i$ and $\mathbf{k} = \mathbf{k}_p - \mathbf{k}_i$, where \mathbf{k}_p is the wave vector in the medium of the pumping wave of frequency ω_p and \mathbf{k}_i is the wave vector of the Fourier component of frequency ω_i of the fluctuation field.

To find the field radiated into the vacuum by the nonlinear polarization we introduce a rectangular coordi-

nate system (see Fig. 1) with the xy plane in the interface between the media and the z axis directed from the medium into the vacuum. Let \mathbf{k}_s be the wave vector of the scattered wave ($k_s = \omega/c$). We choose the x axis so that \mathbf{k}_s will lie in the yz plane, and denote the angles between the z axis and the wave vectors in vacuo of the scattered and pumping waves by θ_s and θ_p , respectively.

Finding the amplitudes of the scattered radiation reduces to solving Maxwell's equations with the source (1) under the boundary condition that the tangential components of the electric and magnetic field vectors be continuous at the interface between the media. Standard calculations^{9,11} yield the following expressions for the amplitudes of the s and p components of the scattered waves:

$$\begin{aligned} E_{\perp} &= 4\pi k_s P_{1\omega} \{ |\cos \theta_s + (\epsilon_s - \sin^2 \theta_s)^{1/2}| [k_s - k_s (\epsilon_s - \sin^2 \theta_s)^{1/2}] \}^{-1} = f_1 P_{1\omega}, \\ E_{\parallel} &= 4\pi k_s [P_{2\omega} (\epsilon_s - \sin^2 \theta_s)^{1/2} + P_{3\omega} \sin \theta_s] \\ &\times \{ |\epsilon_s \cos \theta_s + (\epsilon_s - \sin^2 \theta_s)^{1/2}| [k_s - k_s (\epsilon_s - \sin^2 \theta_s)^{1/2}] \}^{-1} = f_2 P_{2\omega} + f_3 P_{3\omega}, \end{aligned} \quad (2)$$

in which the $P_{m\omega}$ ($m=1, 2, 3$) are the projections of the vector \mathbf{P}_{ω} onto the coordinate axes; $k_3 = -k_p \cos \theta'_p - k_i \cos \theta_i$, where $n \sin \theta'_p = \sin \theta_p$, n being the refractive index at the pumping frequency; and θ_i is the angle between the vector \mathbf{k}_i and the z axis. We have denoted the functions of the angle variables by f_m ($m=1, 2, 3, \dots$). The boundary conditions require the tangential components of \mathbf{k} and \mathbf{k}_s to be equal, and this leads to the following formula relating the solid angles for the scattered wave and ballast wave:

$$k_i^2 |\cos \theta_i| dO_i = k_s^2 \cos \theta_s dO_s. \quad (3)$$

The spectral density of the light flux is given by

$$dI_{m\omega_s} = \frac{c}{2\pi} f_m^2 \chi_m^2 E_0^2 |E_i|^2 dN, \quad (4)$$

where the χ_m ($m=1, 2, 3$) are the nonlinearity constants and dN is the number of field oscillators emitting radiation in a unit spectral interval into the solid angle dO_s . These same oscillators contribute to the energy flux at frequency ω_i :

$$\frac{cn_i}{2\pi} |E_i|^2 dN = u_{\omega_i} \frac{d\omega_i}{dk_i} \frac{dO_i}{4\pi}, \quad (5)$$

where n_i is the refractive index at frequency ω_i and u_{ω_i} is the spectral density of the electromagnetic energy of the fluctuation field.¹⁰ Determining dN from (5), bearing in mind that at a fixed angle θ_s two groups of oscillators, differing in the sign of $\cos \theta_i$, contribute to the light flux (4), and making use of Eq. (3), we obtain the desired formula

$$\frac{dI_{m\omega_s}}{dO_s} = I_0 \chi_m^2 (f_m^2 + f_m^2) \frac{\hbar \omega_i \omega_s^2}{4\pi^2 c^2 n_i} \operatorname{cth} \left(\frac{\hbar \omega}{2kT} \right) \frac{\cos \theta_s}{|\cos \theta_i|}. \quad (6)$$

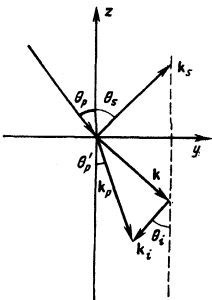


FIG. 1. Orientation of the wave vectors of the interacting fields with respect to the interface between the media.

Here I_0 is the pumping-light flux and the subscripts + and - on the functions f correspond to the different signs of $\cos \theta_i$ ($\cos \theta_i = \pm |\cos \theta_i|$).

It follows from the boundary conditions [see Eq. (4)] that for each fixed frequency there is a cone of directions ($\sin^2 \theta_i \leq 1$) within which there is radiation of frequency ω_s . In the special case of normal incidence of the pumping wave these directions are those for which

$$\sin \theta_s \leq n_i (\omega_p - \omega_s) / \omega_s.$$

Formula (6) gives an infinite spectral intensity at the boundary of the cone; this is an obvious consequence of neglecting the absorption of the light waves. Experimentally one registers the scattered radiation within a finite angular interval $\Delta \theta_s$, i.e., one does not measure the derivative of the function, but its increment, and the latter is always finite.

Let us illustrate what was said above for the case in which the propagation direction of the pumping light is perpendicular to the interface between the media. In this case, for the region near the boundary of the cone we have

$$\frac{\cos \theta_s}{\cos \theta_i} \approx -n_i \frac{\omega_i}{\omega_s} \frac{d}{d\theta_s} \cos \theta_i.$$

The small conversion factor sets a lower bound to the choice of $\Delta \theta_s$. In the experiments described below, $\Delta \theta_s$ was of the order of 4° and the corrections associated with absorption could not be registered ($\Delta \theta_s \gg \epsilon''/\epsilon'$).

Experimentally, it is convenient to vary the orientation of the crystal without changing the positions of the pumping source and the detecting system. In our experiments the vectors \mathbf{k}_s and \mathbf{k}_p were orthogonal to one another and lay in the plane of incidence ($\theta_p = (\pi/2) - \theta_s$). It follows from formula (6) that on rotating the crystal one should observe two maxima in the spectral intensity of the scattered light. The positions of the maxima correspond to the vanishing of $\cos \theta_i$. The corresponding angles can be found from the equation

$$\omega_p \cos \theta_s - \omega_s \sin \theta_i = n_i (\omega_p - \omega_s). \quad (7)$$

EXPERIMENTAL SETUP AND MEASURING TECHNIQUE

The fact that the pumping wave is converted to the scattered radiation of interest with so small a conversion factor made it necessary to use photon counting techniques in the experiment. Figure 2 is a block diagram of the apparatus. The radiation from the LTIPCh-7 laser 1 falls onto the specimen 4 (a thin plate of LiIO_3) on a Fedorov stand. The normal to the specimen lay in the plane of the wave vectors of the pumping and scattered radiations. In the experiment we measured the intensity of the signal as a function of the angle between the wave vector of the pumping light and the normal to the specimen. In front of the specimen was a set of filters which cut off the radiation at a wavelength of $1.06 \mu\text{m}$. The radiation scattered at 90° first passed through an SPN-2 double monochromator and then through a set of filters 3 that cut off the second harmonic radiation ($0.53 \mu\text{m}$), and finally entered the photomultiplier 6. The photomultiplier was mounted in a light-tight housing

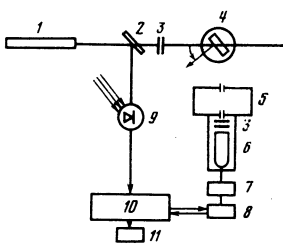


FIG. 2. Experimental setup: 1—laser, 2—glass beam splitter, 3—filters, 4—specimen on a Fedorov stand, 5—monochromator, 6—photomultiplier in a light tight housing, 7—amplifier, 8—coincidence circuit, 9—photodiode, 10—minicomputer, 11—digital display.

joined to the double monochromator and was calibrated with an STsV incandescent lamp whose spectrum was known. The photomultiplier signal was fed through the amplifier 7 to the coincidence circuit 8 with a constant delay of about 40 nsec. To trigger the coincidence circuit, part of the laser beam was diverted by a glass beam splitter 2 and was directed onto a photodiode 9. The pulse from the photodiode 9 triggered the minicomputer 10, which controlled the coincidence circuit and registered the count rate. A variable delay line made it possible to vary the difference between the arrival times of the signal and gating pulses at the coincidence circuit from zero to ± 80 nsec. The size of the pulse sample could be reduced in unit steps from a maximum of 1024. The signal-pulse count was displayed on the digital display 11. The ratio of the number in the display to the size of the pulse sample gave the event rate.

The spectrum was recorded over the range from 0.5 to $1 \mu\text{m}$. The choice of this range was dictated by the spectral sensitivity of the photomultiplier and the transmission characteristics of the interference filters. The noise level of the recording system was 2–3 noise photoelectrons in 200 flashes. When measuring the signal, some 20 to 80 photoelectrons were recorded in 200 flashes. During the experiment the size of the pulse sample was varied from 200 to 1000. The laser operated at a repetition rate of 25 flashes/sec. The laser pulse was about 10^{-8} sec long and had an energy of 0.002 J.

When measuring the angular dependence of the scattered radiation the monochromator was replaced by an interference filter to increase the luminosity. For angular discrimination we mounted two diaphragms (dioptr) in front of the filter; these provided a view angle of 4° .

Tests using filters of known transmission showed that the system operated linearly; the signal-pulse rate can therefore be regarded as proportional to the intensity of the scattered radiation in the spectral interval defined by the monochromator. The reliability of the cutoff filters was tested in a special control experiment. The monochromator was adjusted to the pumping wavelength and the intensity of the scattered light was measured. Under these conditions the signal fell to the noise level, indicating that the cutoff filters operate reliably. The wavelength of the observed signal was identified in a second control experiment. A filter that was opaque to

the observed frequency but transparent to the pumping frequency was placed between the specimen and the recording system. Again the signal fell to the noise level, indicating the absence of luminescence emitted by elements of the system under the action of the pumping light.

The above tests showed without doubt that the source of the signal is neither pumping light that might have leaked into the photomultiplier nor luminescence excited by the pumping light in elements of the recording system, but is indeed radiation coming from the crystal.

In addition to experiments in which we evaluated the instrumental effects and the noise level, we made a number of tests to establish the parametric character of the observed scattered radiation.

1) We measured the spectral characteristics of the scattered radiation and compared the envelop of the spectrum with the spectral distribution of spontaneous PL. The second harmonic from a ruby laser was used for pumping. The experiments showed that the spectra of the two processes are identical (in the absence of absorption). The spectral brightness was four orders of magnitude lower for the scattering than for the spontaneous PL.

2) The shape of the scattered-radiation pulse was determined by varying the delay time. It was found that the scattering is prompt (within the ~ 5 nsec time resolution of the system).

3) The intensity of the signal at $0.6 \mu\text{m}$ wavelength was measured as a function of temperature, using the second harmonic from an yttrium aluminum garnet (YAG) laser for pumping. Then, without altering the temperature of the specimen, the LTIPCh-7 doubler was turned off and the intensity of the second harmonic ($\lambda = 0.53 \mu\text{m}$) produced out of synchronism by conversion of the YAG laser light ($\lambda = 1.06 \mu\text{m}$) in the investigated crystal was measured. The temperature dependence of the intensities of the investigated radiation and the second harmonic were always similar; this provides additional evidence that the two phenomena are similar in nature.

RESULTS

Several series of lithium iodate crystal specimens were used in the experiments. The crystals were grown from aqueous solutions having various degrees of acidity. Specimens of α -LiIO₃ crystals were used in the experiments; these crystals belong to class 6 of the hexagonal system, and the components of their nonlinear-susceptibility tensor are of the order of 10^{-8} esu. There were also a few specimens of β -LiIO₃; these crystals belong to the tetragonal system and have a center of symmetry.

The density of inclusions with sizes of the order of $10 \mu\text{m}$ and larger was determined visually with the aid of a microscope; it ranged from 18 to 560mm^{-3} , depending on the specimen. Plates 2.8 mm thick were cut from the crystals. Specimens of two types were used: *z*-cut specimens with the normal to the large face

parallel to the optical axis, and y -cut specimens with the normal perpendicular to the axis. The specimens were so oriented with respect to the pumping beam that the polarization of the beam made a right angle with the optical axis of the crystal. With this geometry no spontaneous PL is excited because the conditions for phase matching are not satisfied.

Figure 3 shows a number of spectra of the scattered radiation measured with different lithium iodate specimens. Curves 1 and 3-7 were obtained with α -LiIO₃ crystals, while curve 2 was obtained with a β -LiIO₃ crystal. The investigated specimens had a tetragonal habit and optically they were highly nonuniform. X-ray diffraction studies revealed that the nonuniformity was due to inclusions of the α -phase.

It is evident from these results (see Fig. 3) that the scattered radiation has a broad spectrum lying in the Stokes region with respect to the pumping frequency. The intensity of the scattering increases with increasing concentration of inclusions with sizes of the order of or larger than 10 μm .

Analysis of the curves reveals a connection between the absorption coefficient for the idle wave and the spectral envelope of the scattered radiation. In Fig. 4, starting from the absorption coefficient $k(\omega_i)$ at the idle frequency for one of the specimens, we have constructed the relation

$$I(\omega_s) \sim \omega_s^2 k(\omega_p - \omega_s).$$

We obtained similar results for other specimens, and also on changing the pumping wavelength (by using the radiation from a ruby laser).

Study of the polarization characteristics of the radiation using a Glan prism showed that both the intensity of the scattered light at a fixed wavelength and the integral intensity of the scattered light were independent of the angular setting of the polarizer. In other words, the scattered light has no particular polarization direction.

The surface of the specimen and defects with sizes of $\sim 10 \mu\text{m}$ or larger make comparable contributions to the intensity of the scattered light; this indicates that the scattered radiation is formed at interfaces between the media. To test this hypothesis we investigated the angular distribution of the scattered radiation at wavelengths of 0.65 and 0.6 μm for thin plates 2.8 mm thick. Figure 5 shows the intensity of the scattered light at 0.65 μm

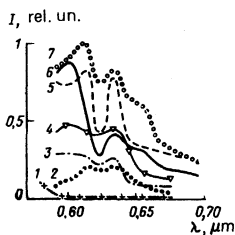


FIG. 3. Spectral distributions of the scattered radiation from different specimens. The curves are numbered in order of increasing inclusion density. Curves 1, 4, 5, and 7 are for y -cut specimens, and curves 3 and 6, for z -cut specimens. Curve 2 is for the β phase.

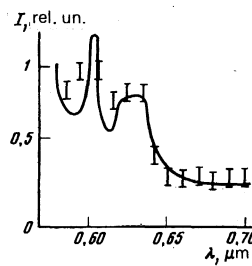


FIG. 4. Relation between the absorption coefficient for the idle wave and the spectral envelope of the scattered radiation. The full curve was constructed from the experimental frequency dependence of the absorption coefficient in the infrared.

wavelength as a function of the angle between the normal to the surface of the specimen and the propagation direction of the pumping wave. Large maxima are observed at angles of 26 and 56°. The angles calculated with Eq. (7) for the idle frequency are 23.9 and 54.5° for the ordinary wave and 25 and 53.3° for the extraordinary wave. These angles are marked by vertical lines in Fig. 5. Similar measurements were made at a wavelength of 0.6 μm . The experimental values of the angles at which maxima were observed in the intensity of the scattered light as a function of the incidence angle of the pumping wave were 30 and 52°. The corresponding theoretical values are 32.2 and 50.7° for the ordinary wave and 32.8 and 50° for the extraordinary wave.

CONCLUSION

The experimental results obtained in this study allow us to conclude that the phenomenon we were investigating actually was parametric scattering of light at interference between media. The experimental data available to us indicate that this type of scattering is sensitive to the structure of the specimen. Scattering was observed not only in the lithium iodate crystals discussed above, but also in a number of other crystals; LiNbO₃, CdS, and ZnSe. The physical causes responsible for the presence of the inhomogeneities are different in these cases. It may be supposed that scattering of the type discussed here will find application in crystal structure research.

The authors thank S. A. Akhmanov for discussing the work.

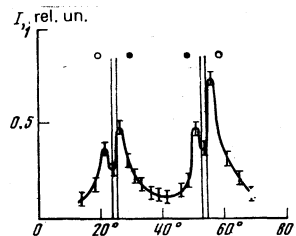


FIG. 5. Indicatrix of the scattered radiation of wavelength 0.65 μm when pumping with 0.53 μm light.

¹S. E. Harris, M. K. Oshman, and R. L. Byer, *Phys. Rev. Lett.* **18**, 732 (1967).
²D. N. Klyshko and D. P. Krindach, *Zh. Eksp. Teor. Fiz.* **54**, 697 (1968) [*Sov. Phys. JETP* **27**, 371 (1968)].
³T. G. Giallorenzi and C. L. Tang, *Phys. Rev.* **166**, 225 (1968).
⁴D. N. Klyshko, *Zh. Eksp. Teor. Fiz.* **55**, 1006 (1968) [*Sov. Phys. JETP* **28**, 522 (1969)].
⁵L. I. Mandel'shtam, *Polnoe sobranie trudy* (Complete Collected Works), Vol. 1, Izd. AN SSSR, 1948, p. 109.
⁶S. N. Kosolobov and R. I. Sokolovsky, *Optical Commun.* **23**, 128 (1977).
⁷D. V. Sivukhin, *Lektsii po fizicheskoi optike* (Lectures on Physical Optics), Part 1, Izd. NGU, Novosibirsk, 1968, p. 223.

⁸S. A. Akhmanov and R. V. Khokhlov, *Problemy nelineinoi optiki* (Problems of Nonlinear Optics), Izd. AN SSSR, 1964.
⁹N. Blombergen, *Nonlinear optics*, Benjamin, 1965 (Russ. Transl. "Mir", 1966).
¹⁰L. D. Landau and E. M. Lifshitz, *Élektrodinamika sploshnykh sred* (Electrodynamics of Continuous Media), Section 91, Fizmatgizdat, 1959 (Engl. Transl. Pergamon, 1959).
¹¹S. M. Rytov, *Teoriya élektricheskikh fluktuatskii i teplovogo izlucheniya* (Theory of Electrical Fluctuations and Thermal Radiation), Izd. AN SSSR, 1953.

Translated by E. Brunner

Splitting and coalescence of photons on a hydrogenlike atom

L. F. Vitushkin, E. G. Drukarev, and A. I. Mikhaïlov

V. P. Konstantinov Institute of Nuclear Physics, USSR Academy of Sciences, Leningrad
 (Submitted 30 June 1978)
Zh. Eksp. Teor. Fiz. **76**, 824-834 (March 1979)

At photon energies $\omega \ll m$ and in certain kinematic regions near $\omega \gtrsim m$, the splitting and coalescence of photons on an atom are due to their interaction with bound electrons. The amplitude, the angular and energy distributions, and the total cross section are calculated for all these cases. The calculations are performed for a hydrogenlike atom, but the principal estimates are valid for any atom.

PACS numbers: 32.80. - t

1. INTRODUCTION

Splitting of a photon into two photons can occur in the Coulomb field of a nucleus, and also when photons interact with bound electrons. If the final and initial states of the atom coincide, then the amplitude of the photon splitting on the atom can be represented in the form

$$F = F_0 + F_1, \quad (1)$$

where F_0 and F_1 are the nuclear and electronic parts of the amplitude. They are expressed by the Feynman diagrams shown in Figs. 1a and 1b, with all possible permutations of the photons. All the foregoing applies also to coalescence of two photons into one. These two processes will be considered together.

The splitting of photons in the field of a nucleus was first considered more than 40 years ago by Williams.¹ An exact expression for the amplitude of this process was derived by Shima.² Constantini *et al.*³ investigated both the splitting and the coalescence of photons in the field of a nucleus. Various limiting cases were also investigated.⁴⁻¹⁰

In this paper we consider splitting and coalescence of photons on an atom. We calculate the amplitude and the cross sections for all the cases in which the main contribution to the amplitude is made by its electronic part

F_1 . It will be shown that if all the photon energies $\omega_i \ll m$ (m is the electron mass; $\hbar = c = 1$), then $F_0 \ll F_1$. At $\omega_i \gtrsim m$ the total splitting cross section is determined by the "nuclear" term F_0 of the amplitude. In certain kinematic regions, however, the amplitude F_1 makes the main contribution to the differential cross section of the splitting or to the total cross section of the coalescence of the photons.

All the calculations are made for the ground state of a hydrogenlike atom, but the main estimates are valid for any atom. It is assumed that the charge Z of the nucleus

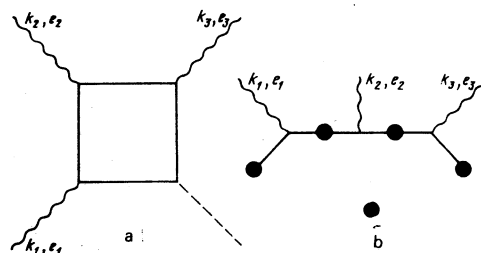


FIG. 1. Feynman diagrams of the amplitude of splitting of one photon into two and of coalescence of two photons into one on an atom. The dark blocks denote the Coulomb field. The dashed line corresponds to the Fourier component of the Coulomb field.